Journal of Statistical Physics, Vol. 128, Nos. 1/2, July 2007 (© 2007)
DOI: 10.1007/s10955-006-9182-z

Effects of Noise on Ecological Invasion Processes: Bacteriophage-Mediated Competition in Bacteria

Jaewook Joo,[1] Eric Harvill,[2] and Réka Albert[3]

Received January 14, 2006; accepted July 18, 2006
Published Online September 12, 2006

Pathogen-mediated competition, through which an invasive species carrying and transmitting a pathogen can be a superior competitor to a more vulnerable resident species, is one of the principle driving forces influencing biodiversity in nature. Using an experimental system of bacteriophage-mediated competition in bacterial populations and a deterministic model, we have shown in Joo *et al.* [*Proc. R. Soc. B* **273**,1843–1848 (2006)] that the competitive advantage conferred by the phage depends only on the relative phage pathology and is independent of the initial phage concentration and other phage and host parameters such as the infection-causing contact rate, the spontaneous and infection-induced lysis rates, and the phage burst size. Here we investigate the effects of stochastic fluctuations on bacterial invasion facilitated by bacteriophage, and examine the validity of the deterministic approach. We use both numerical and analytical methods of stochastic processes to identify the source of noise and assess its magnitude. We show that the conclusions obtained from the deterministic model are robust against stochastic fluctuations, yet deviations become prominently large when the phage are more pathological to the invading bacterial strain.

KEY WORDS: phage-mediated competition, invasion criterion, Fokker-Planck equation, stochastic simulations

1. INTRODUCTION

Theoretical studies of ecological processes generally employ either deterministic or stochastic modeling approaches. In the former case, the evolution of a

[1] Department of Physics, Pennsylvania State University, University Park, PA 16802, USA. e-mail: jjoo@phys.psu.edu.
[2] Department of Veterinary and Biomedical Sciences, Pennsylvania State University, University Park, PA 16802, USA.
[3] Department of Physics and Huck Institute of the Life Sciences, Pennsylvania State University, University Park, PA 16802, USA.

population is described by (partial-) differential or difference equations.[1] In the latter case, the population is modeled as consisting of discrete entities, and its evolution is represented by transition probabilities. While the deterministic modeling approach has been favored and widely applied to ecological processes due to its simplicity and well-established analytic tools,[1] its applicability is limited in principle to a system with no fluctuations and no (spatial) correlations, e.g., a system composed of a large number of individuals under rapid mixing. Being more realistic representations of noisy ecological systems, the stochastic models have been studied in the context of the stochastic interacting particle system,[2,3] in the mathematical epidemiology,[4–7] and in the stochastic population biology.[8–10] The stochastic modeling approach has, however, its own downside: most stochastic models are analytically intractable and stochastic simulation, a popular alternative, is demanding in terms of computing time. Nonetheless, the stochastic modeling approach is indispensable when a more thorough understanding of an ecological process is pursued.

Apparent competition, the competitive advantage conferred by a pathogen to a less vulnerable species, is generally accepted as a major force influencing biodiversity.[11–14] Due to the complexities originating from dynamical interactions between multiple hosts and pathogens, it has been difficult to single out and to quantitatively measure the effect of pathogen-mediated competition in nature or laboratory.[12–19] A system of bacteria and bacteriophage, however, enables us to overcome these difficulties; it is relatively easy to eliminate direct resource competition, to measure the parameter values of the system, and even to manipulate both host resistance mechanisms and pathogen virulence. The bacteria-phage infection system is therefore one of the most suitable systems for the exploration of pathogen-mediated competition. Moreover, studying this system can provide insights on the role of bacteriophage in the formation of microbial communities.[20]

In our previous work[21] we developed an experimental system and a theoretical framework for studying bacteriophage-mediated competition in bacterial populations. The experimental system consisted of two genetically identical bacterial strains; they differed in that one strain was a carrier of the bacteriophage and resistant to it while the other strain was susceptible to phage infection (see Table I). Based on the *in vitro* experimental set-up, we constructed a differential equation model of phage-mediated competition between the two bacterial strains. Most model parameters were measured experimentally, and a few unknown parameters were estimated by matching the time-series data of the two competing populations to the experiments (see Table II and Fig. 1). The model predicted, and experimental evidence confirmed, that the competitive advantage conferred by the phage depends only on the relative phage pathology and is independent of other phage and host parameters such as the infection-causing contact rate, the spontaneous and infection-induced lysis rates, and the phage burst size.

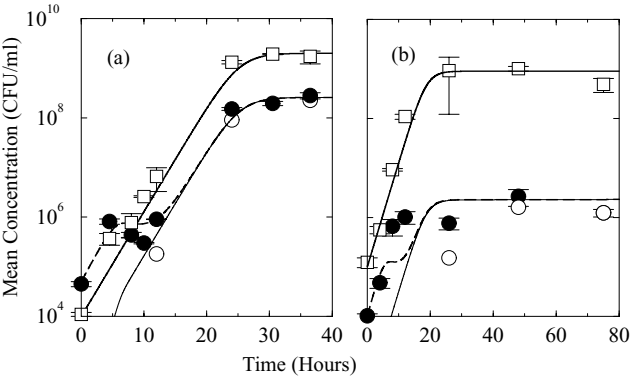

Fig. 1. Illustrations of phage-mediated competition obtained from *in vitro* experiments (symbols) and a deterministic model (lines). The phage infection system consists of two genetically identical Bordetella bronchiseptica bacteria (Bb) and the bacteriophage BPP-1 (Φ).[21] A gentamicin marker (Gm) is used to distinguish the susceptible bacterial strain (BbGm) from the phage-carrying bacterial strain (Bb::Φ). As time elapses, a fraction of BbGm become lysogens (BbGm::Φ) due to the phage-infection process. Bb::Φ are represented by open squares and a thick solid line, BbGm::Φ by open circles and a thin solid line, and the total BbGm (BbGm+BbGm::Φ) by filled circles and a long-dashed line, respectively. (a) Lysogens (Bb::Φ) exogenously and endogenously carrying the prophage invade the BbGm strain susceptible to phage, and (b) lysogens (Bb::Φ) are protected against the invading susceptible bacterial strain (BbGm).[21] The differential equations were solved with biologically relevant parameter values. (See Sec. 3.1 and Tables I and II for a detailed description.)

In a typical bacteriophage-mediated invasion process, the initial population size of the invading bacterial strain is likely to be small. Therefore the stochastic fluctuations of the bacterial population size are expected to be large and are likely to affect the outcome of phage-mediated competition. To better understand the role of phage-mediated competition in microbial communities, and to test the generality of the conclusions of the deterministic model,[21] here we investigate the effects of noise on phage-mediated competition. The phage-bacteria infection system is modeled and analyzed with two probabilistic methods: (i) a linear Fokker-Planck equation obtained by a systematic expansion of a full probabilistic model (i.e., a master equation), and (ii) stochastic simulations. Both probabilistic methods are used to identify the source of noise and assess its magnitude, through determining the ratio of the standard deviation to the average population size of each bacterial strain during the infection process. Finally stochastic simulations show that the conclusions obtained from the deterministic model are robust against stochastic fluctuations, yet deviations become large when the phage are more pathological to the invading bacterial strain.

Table I. Notations and Characteristics for Bacterial Strain and Phage Used in this Study

Notations	Chracteristics
Bb	Wild-type bronchiseptica bacterial strain.[22]
BbGm	Bb with a gentamicin antibiotic marker.[23]
Bb::Φ	Bb containing a prophage (lysogen), which is resistant to Φ.[23]
BbGm::Φ	Bb with a gentamicin antibiotic marker and containing a prophage, which is resistant to Φ.[23]
BPP-1 Φ	Lysogenic phage[23]
S	Susceptible bacteria, ready to be infected through contact with Φ.
L	Latent bacteria in an interim state between phage infection and bacterial lysis. The phage replicates and then lyses latent bacteria after an incubation period $1/\lambda$, during which the latent bacteria do not divide.
I	Lysogenic bacteria carrying lysogenic phage (Φ) in their genome. Lysogenic bacteria grow, replicating lysogenic phage (Φ) as a part of the bacterial chromosome, and are resistant to Φ.

Table II. Parameters Used for the Numerical Simulation of the Phage-Mediated Competition in *B. bronchiseptica*

Parameter	Name	Range	Resources
a	(Free) growth rate	0.54	Measured[21]
δ	Spontaneous lysis rate	$0 \leq \delta < a$	Measured[21]
λ	ϕ-induced lysis rate	0.08–0.17	Measured[21]
χ	Burst size	10–50	Measured[21]
P	Phage pathology	$0 \leq P \leq 1$	Estimated
κ	Contact rate	$\kappa > 0$	Estimated
$N_{\max}$	Holding capacity	$\sim 10^9$	Measured[21]

Note. The two undetermined parameters P and κ [(hours·CFU/ml)$^{-1}$] were estimated by comparing the experimental results with those of the theoretical model and by minimizing discrepancies.

2. A MODEL OF PHAGE-MEDIATED COMPETITION IN BACTERIA

The system under our consideration consists of two strains of bacteria: both bacterial strains are susceptible to phage infection and one invasive bacterial strain contains phage.[21] Two bacterial strains are genetically identical except in their susceptibilities to phage and in phage pathologies on them. We restricted the infection system such that bacteria grow in a log phase, i.e., there is no resource competition between them. The interactions involved in this phage-mediated competition between two bacterial strains are provided diagrammatically in Fig. 2.

We model this dynamically interacting system with seven homogeneously mixed subpopulations: Each bacterial strain can be in one of susceptible (S_j), lysogenic (I_j), or latent (L_j) states, and they are in direct contact with bacteriophage (Φ). All bacteria divide with a constant rate when they are in a log growth phase, while their growth is limited when in stationary phase. Thus we assume that the bacterial population grows with a density-dependent rate $r(\Omega) = a(1 - \Omega/\Omega_{\max})$ where Ω is the total bacterial population and $\Omega_{\max}$ is the maximum number of bacteria supported by the nutrient broth environment. Susceptible bacteria (S_j) are uninfected and become infected through contact with phage at a rate κ_j. Lysogenic bacteria (I_j) carry lysogenic phage (Φ), which incorporate their genome into the bacterial genome, and grow, replicating lysogenic phage (Φ) as part of the bacterial chromosome, and are resistant to phage. Even though these lysogens (I_j) are very stable without external perturbations, spontaneous induction can occur at a low rate δ, consequently replicating the phage and lysing the host bacteria. Latent bacteria (L_j) are in an interim state between phage infection and bacterial lysis, and the phage replicate and then lyse the host bacteria after an incubation period $1/\lambda$, during which the bacteria do not divide.[24] Upon infection the lysogenic phage (Φ) can either take a lysogenic pathway or a lytic pathway, stochastically determining the fate of the infected bacterium.[24] We assume that a fraction P_j

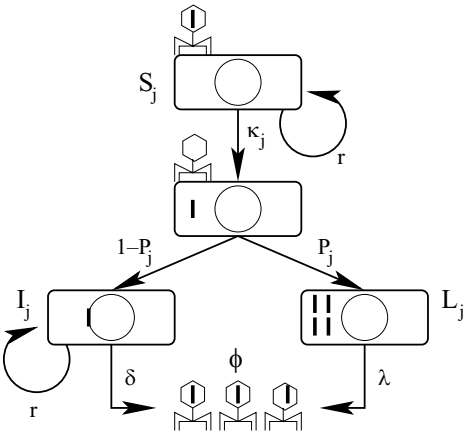

Fig. 2. Diagrammatic representation of phage-mediated competition between two bacterial strains with different susceptibilities κ_j and phage pathogenicities P_j. The subscript $j \in \{1, 2\}$ denotes the type of bacterial strain. Phage (Φ) are represented by hexagons carrying a thick segment (Φ DNA). A susceptible bacterium (S_j) is represented by a rectangle containing an inner circle (bacterial DNA) while a lysogen (I_j) is represented by a rectangle containing Φ DNA integrated into its bacterial DNA. All bacterial populations grow with an identical growth rate r while a latent bacterium (L_j) is assumed not to divide. δ and λ represent spontaneous and infection-induced lysis rates, respectively.

of infected bacteria enter a latent state (L_j) while the phage lysogenize a fraction $1 - P_j$ of their hosts, which enter a lysogenic state (I_j). Thus the parameter P_j characterizes the pathogenicity of the phage, incorporating multiple aspects of phage-host interactions resulting in damage to host fitness. In general, both the number of phage produced (the phage burst size χ) and the phage pathology P_j depend on the culture conditions.[24] The two bacterial strains differ in susceptibility (κ_j) and vulnerability (P_j) to phage infection.

When the initial population size of the invading bacterial strain is small, the stochastic fluctuations of the bacterial population size are expected to be large and likely to affect the outcome of the invasion process. A probabilistic model of the phage infection system is able to capture the effects of intrinsic noise on the population dynamics of bacteria. Let us define the joint probability density $P_t(\underline{\eta})$ denoting the probability of the system to be in a state $\underline{\eta}(t) = (S_1, I_1, L_1, S_2, I_2, L_2, \Phi)$ at time t where S_j, I_j and L_j denote the number of bacteria in susceptible, latent or infected states, respectively. The time evolution of the joint probability is determined by the transition probability per unit time $T(\underline{\eta}'|\underline{\eta}; t)$ of going from a state $\underline{\eta}$ to a state $\underline{\eta}'$.[25,26] We assume that the transition probabilities do not depend on the history of the previous states of the system but only on the immediately past state. There are only a few transitions that are allowed to take place. For instance, the number of susceptible bacteria increases from S_1 to $S_1 + 1$ through

the division of a single susceptible bacterium and this process takes place with the transition rate $T(S_1+1, I_1, L_1, S_2, I_2, L_2, \Phi | S_1, I_1, L_1, S_2, I_2, L_2, \Phi) = r(\Omega)S_1$. The allowed transition rates are

$$\begin{aligned}
&T(S_j+1, \ldots | S_j, \ldots; t) = r(\Omega)S_j,\\
&T(\ldots, I_j+1, \ldots | \ldots, I_j, \ldots; t) = r(\Omega)I_j,\\
&T(S_j-1, I_j+1, \ldots, \Phi-1 | S_j, I_j, \ldots, \Phi; t) = \kappa_j(1-P_j)\Phi S_j \qquad (1)\\
&T(S_j-1, \ldots, L_j+1, \Phi-1 | S_j, \ldots, L_j, \Phi; t) = \kappa_j P_j \Phi S_j\\
&T(\ldots, I_j-1, \ldots, \Phi+\chi | \ldots, I_j, \ldots, \Phi; t) = \delta I_j\\
&T(\ldots, L_j-1, \ldots, \Phi+\chi | \ldots, L_j, \ldots, \Phi; t) = \lambda L_j
\end{aligned}$$

where $\Omega(t) = \sum_j (S_j(t) + I_j(t) + L_j(t))$. The second line represents the division of a lysogen; the 3rd line describes an infection process by phage taking a lysogenic pathway while the fourth line denotes an infection process by phage taking a lytic pathway. The last two transitions are spontaneously-induced and infection-induced lysis processes, respectively. Bacterial subpopulations that are unchanged during a particular transition are denoted by "...". The parameters a, k_j, δ and λ in the transition rates of Eq. (1) represent the inverse of the expected waiting time between events in an exponential event distribution and they are equivalent to the reaction rates given in Fig. 2.

The stochastic process specified by the transition rates in Eq. (1) is Markovian, thus we can immediately write down a master equation governing the time evolution of the joint probability $P(\underline{\eta})$.[25,26] The rate of change of the joint probability $P_t(\underline{\eta})$ is the sum of transition rates from all other states $\underline{\eta'}$ to the state $\underline{\eta}$, minus the sum of transition rates from the state $\underline{\eta}$ to all other states $\underline{\eta'}$:

$$\begin{aligned}
&\frac{dP_t(\underline{\eta})}{dt}\\
&= \sum_j \Big\{ \big(E_{S_j}^{-1} - 1\big)[T(S_j+1, \ldots | S_j, \ldots; t)P_t(\underline{\eta})\\
&\quad + \big(E_{I_j}^{-1} - 1\big)[T(\ldots, I_j+1, \ldots | \ldots, I_j, \ldots; t)P_t(\underline{\eta})]\\
&\quad + \big(E_{\Phi}^{+1}E_{S_j}^{+1}E_{I_j}^{-1} - 1\big)[T(S_j-1, I_j+1, \ldots, \Phi-1 | S_j, I_j, \ldots, \Phi; t)P_t(\underline{\eta})]\\
&\quad + \big(E_{\Phi}^{+1}E_{S_j}^{+1}E_{L_j}^{-1} - 1\big)[T(S_j-1, \ldots, L_j+1, \Phi-1 | S_j, \ldots, L_j, \Phi; t)P_t(\underline{\eta})]\\
&\quad + \delta\big(E_{I_j}^{+1}E_{\Phi}^{-\chi} - 1\big)[T(\ldots, I_j-1, \ldots, \Phi+\chi | \ldots, I_j, \ldots, \Phi; t)P_t(\underline{\eta})]\\
&\quad + \lambda\big(E_{L_j}^{+1}E_{\Phi}^{-\chi} - 1\big)T(\ldots, L_j-1, \ldots, \Phi+\chi | \ldots, L_j, \ldots, \Phi; t)P_t(\underline{\eta})]\Big\}
\end{aligned} \qquad (2)$$

where $E_\alpha^{\pm 1}$ is a step operator which acts on any function of α according to $E_\alpha^{\pm 1} f(\alpha, \ldots) = f(\alpha \pm 1, \ldots)$.

The master equation in Eq. (2) is nonlinear and analytically intractable. There are two alternative ways to seek a partial understanding of this stochastic system: a stochastic simulation and a linear Fokker-Planck equation obtained from a systematic approximation of the master equation.[25–27] A stochastic simulation is one of the most accurate/exact methods to study the corresponding stochastic system.[27] However, stochastic simulations of an infection process in a large system are very demanding in terms of computing time, even today. Moreover, simulation studies can explore only a relatively small fraction of a multi-dimensional parameter space, thus provide neither a complete picture nor intuitive insight to the current infection process. The linear Fokker-Planck equation is only an approximation of the full stochastic process; it describes the time-evolution of the probability density, whose peak is moving according to macroscopic equations.[25,26] In cases where the macroscopic equations are nonlinear, one needs to go beyond a Gaussian approximation of fluctuations, i.e., the higher moments of the fluctuations should be considered. In cases when an analytic solution is possible, the linear Fokker-Planck equation method can overcome most disadvantages of the stochastic simulations. Unfortunately such an analytic solution could not be obtained for the master equation in Eq. (2).

In the following sections we present a systematic expansion method of the master equation to obtain both the macroscopic equations and the linear Fokker-Planck equation, then an algorithm of stochastic simulations.

3. SYSTEMATIC EXPANSION OF THE MASTER EQUATION

In this section we will apply van Kampen's elegant method[25] to a nonlinear stochastic process, in a system whose size increases exponentially in time. This method not only allows us to obtain a deterministic version of the stochastic model in Eq. (2) but also gives a method of finding stochastic corrections to the deterministic result. We choose an initial system size $\Omega_0 = \sum_j (S_j(0) + I_j(0) + L_j(0)) + \Phi(0)$ and expand the master equation in order of $\Omega_0^{-1/2}$. We do not attempt to prove the validity of our application of van Kampen's Ω_0-expansion method to this nonlinear stochastic system; a required condition for valid use of Ω_0-expansion scheme, namely the stability of fixed points, is not satisfied because the system size increases indefinitely and there is no stationary point. However, as shown in later sections, the linear Fokker-Planck equation obtained from this Ω_0-expansion method does provide very reliable results, comparable to the results of stochastic simulations.

In the limit of infinitely large Ω_0, the variables (S_j, I_j, L_j, Φ) become deterministic and equal to $(\Omega_0 s_j, \Omega_0 i_j, \Omega_0 l_j, \Omega_0 \phi)$, where (s_j, i_j, l_j, ϕ) are normalized

quantities, e.g., $s_j = S_j/\Omega_0$. In this infinitely large size limit the joint probability $P_t(\underline{\eta})$ will be a delta function with a peak at $(\Omega_0 s_j, \Omega_0 i_j, \Omega_0 l_j, \Omega_0 \phi)$. For large but finite Ω_0, we would expect $P(\underline{\eta})$ to have a finite width of order $\Omega_0^{1/2}$. The variables (S_j, I_j, L_j, Φ) are once again stochastic and we introduce new stochastic variables $(\xi_{S_j}, \xi_{I_j}, \xi_{L_j}, \xi_\Phi)$: $S_j = \Omega_0 s_j + \Omega_0^{\frac{1}{2}} \xi_{S_j}$, $I_j = \Omega_0 i_j + \Omega_0^{\frac{1}{2}} \xi_{I_j}$, $L_j = \Omega_0 l_j + \Omega_0^{\frac{1}{2}} \xi_{L_j}$, $\Phi_j = \Omega_0 \phi_j + \Omega_0^{\frac{1}{2}} \xi_{\Phi_j}$. These new stochastic variables represent inherent noise and contribute to deviation of the system from the macroscopic dynamical behavior.

The new joint probability density function Π_t is defined by $P_t(\underline{\eta}) = \Pi_t(\underline{\xi})$ where $\underline{\xi} = (\xi_{S_1}, \xi_{I_1}, \xi_{L_1}, \xi_{S_2}, \xi_{I_2}, \xi_{L_2}, \xi_\Phi)$. Let us define the step operators $E_\alpha^{\pm}$, which change α into $\alpha \pm 1$ and therefore ξ_α into $\xi_\alpha + \Omega_0^{-1/2}$, so that in new variables

$$E_\alpha^{\pm 1} = 1 \pm \Omega_0^{-\frac{1}{2}} \frac{\partial}{\partial \xi_\alpha} + \frac{\Omega_0^{-1}}{2} \frac{\partial^2}{\partial \xi_\alpha^2} \pm \cdots \tag{3}$$

The time derivative of the joint probability $P_t(\underline{\eta})$ in Eq. (2) is taken at a fixed state $\underline{\eta} = (S_1, I_1, L_1, S_2, I_2, L_2, \Phi)$, which implies that the time-derivative taken on both sides of $\alpha = \Omega_0 \alpha + \Omega_0^{1/2} \xi_\alpha$ should lead to $d\xi_\alpha/dt = -\Omega_0^{1/2} d\alpha/dt$ where α can be either S_1, I_1, L_1, S_2, I_2, L_2, or Φ. Hence,

$$\frac{dP(\underline{\eta}; t)}{dt} = \frac{\partial \Pi(\underline{\xi})}{\partial t} - \sum_{\alpha = S_1, S_2, I_1, I_2, L_1, L_2, \Phi} \left\{ \Omega_0^{\frac{1}{2}} \frac{\partial \alpha}{dt} \frac{\partial \Pi(\underline{\xi}; t)}{\partial \xi_\alpha} \right\}. \tag{4}$$

We shall assume that the joint probability density is a delta function at the initial condition $\underline{\eta_o}$, i.e., $P_0(\underline{\eta}) = \delta_{\underline{\eta}, \underline{\eta_o}}$.

The full expression of the master equation in the new variables is shown in appendix A. Here we collect several powers of Ω_0. In Sec. 3.1 we show that macroscopic equations emerge from the terms of order $\Omega_0^{1/2}$ and that a so-called invasion criterion, defined as the condition for which one bacterial population outcompetes the other, can be obtained from these macroscopic equations. In Sec. 3.2 we show that the terms of order Ω_0^0 give a linear Fokker-Planck equation whose time-dependent coefficients are determined by the macroscopic equations.

3.1. Emergence of the Macroscopic Equations

There are a few terms of order $\Omega_0^{1/2}$ in the master equation in the new variables as shown in appendix A, which appear to make a large Ω_0-expansion of the master equation improper. However those terms in order of $\Omega_0^{1/2}$ cancel if the following

equations are satisfied

$$\begin{aligned}
\frac{ds_j}{dt} &= r(\Omega)s_j - \kappa_j \Omega_0 \phi s_j \\
\frac{di_j}{dt} &= (1 - P_j)\kappa_j \Omega_0 \phi s_j + (r(\Omega) - \delta) i_j \\
\frac{dl_j}{dt} &= P_j \kappa_j \Omega_0 \phi s_j - \lambda l_j \\
\frac{d\phi}{dt} &= \chi \sum_j (\delta \phi_j + \lambda l_j) - \sum_j \kappa_j \Omega_0 \phi s_j
\end{aligned} \tag{5}$$

Equation (5) are identical to the deterministic equations of the corresponding stochastic model in the limit of infinitely large Ω_0, i.e., in the limit of negligible fluctuations.

These equations allow for the derivation of the *invasion criterion*, defined as the choice of the system parameters in Table II that makes one invading bacterial strain dominant in number over the other strain. Suppose that an initial condition of Eq. (5) is $s_1(0) > 0, s_2(0) > 0, i_1(0) > 0, \phi(0) \geq 0$, and $i_2(0) = l_1(0) = l_2(0) = 0$. (a) In the case of $\phi(0) = \delta = 0$, there is no phage-mediated interaction between bacteria and the ratio of $s_1(t) : s_2(t) : i_1(t)$ remains unchanged for $t \geq 0$. (b) However when either ($\phi(0) = 0$ and $\delta > 0$) or $\phi(0) > 0$, the above ratio changes in time due to phage-mediated interactions. Even though in principle these nonlinear coupled equations are unsolvable, we managed to obtain an analytic solution of the macroscopic Eq. (5) in the limit of a fast infection process, i.e., ($\kappa_j \Omega_0 s_2(0)/a \gg 1$ and $\lambda/a \gg 1$), by means of choosing appropriate time-scales and using a regular perturbation theory.[1] (See Ref. (21) for a detailed description in a simpler system.) We found a simple relationship between the ratios of the two total bacterial populations:

$$r_{12}(t) = r_{12}(0)(1 - P_1)/(1 - P_2) \tag{6}$$

where $r_{12}(t) \equiv \frac{s_1(t)+i_1(t)+l_1(t)}{s_2(t)+i_2(t)+l_2(t)}$ for a sufficiently long time t. Thus the final ratio $r_{12}(t)$ is determined solely by three quantities, the initial ratio, $r_{12}(0)$, and the two phage pathologies, and is independent of other kinetic parameters such as the infection-causing contact rate, the spontaneous and infection-induced lysis rates, and the phage burst size. The invasion criterion, the condition for which bacterial strain 1 outnumbers bacterial strain 2, is simply $r_{12}(t) > 1$.

Figure 3 shows the stationary ratios between the population sizes of two bacterial strains for a generalized deterministic infection system where both bacterial strains are susceptible to phage infection. The simple relationship in Eq. (6), which is represented by the straight diagonal line in Fig. 3, is proven to be true only in the limiting case where the infection process is extremely fast, i.e., susceptible

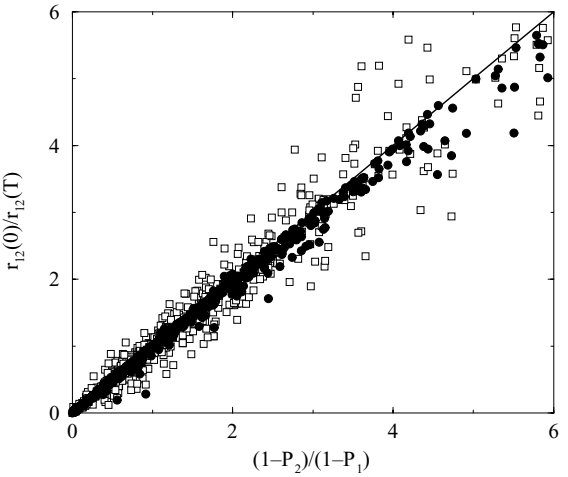

Fig. 3. Numerical verification of the invasion criterion of Eq. (6) for a generalized deterministic infection system where both bacterial strains are susceptible to phage infection. The ratio $r_{12}(0)/r_{12}(T)$ was numerically evaluated by solving Eq. (5) with 2000 sets of parameters chosen uniformly in the intervals $0 < P_1, P_2 < 1$ for phage pathologies, $1/min\{P_1, P_2\} < \chi < 100$ for the phage burst size, $0 < \lambda/a < 0.5$ for the spontaneous induction rate, $10^{-1}s_2(0) < s_1(0) < 10s_2(0)$ and $0 < i_1(0), \phi(0) < 10^{-2}s_2(0)$ for the initial concentrations of bacterial strains and phage. The time T is chosen to be a sufficiently long time. Filled circles represent the data from 1000 sets of parameters with relatively large $\Omega_0\kappa_j s_j/a$ and λ/a (e.g., $0.1 < \Omega_0\kappa_j s_j/a, \lambda/a < 10$). Open circles are from another 1000 sets of parameters with small $\Omega_0\kappa_j s_j/a$ and λ/a (e.g., $0 < \Omega_0\kappa_j s_j/a, \lambda/a < 0.1$).

bacteria are rapidly infected by phage particles and lysed immediately after infection. When the infection process is slow, the stationary ratio could deviate from the simple relationship in Eq. (6) because of its dependence on the kinetic parameters. We validated the invasion criterion of Eq. (6) in the range of both large and relatively small values of $\kappa_j\Omega_0 s_2(0)/a$ and λ/a, by numerically solving Eq. (5) with 2000 sets of parameters selected randomly from the biologically relevant intervals. Figure 3 demonstrates that the simple relationship in Eq. (6) between $r_{12}(0)/r_{12}(t)$ and $(1 - P_2)/(1 - P_1)$ is robust against parameter variations. The results deviate from the linear relationship only for increasing phage pathology on the invading bacterial strain 1 compared with that on bacterial strain 2, i.e., $(1 - P_2)/(1 - P_1) \gg 1$, or $P_1 \gg P_2$.

3.2. Linear Noise Approximation: A Linear Fokker Planck Equation

For simplicity we will assume hereafter that all bacteria grow with a growth rate $r = a$ in a log phase, i.e., there is no resource competition. Identifying terms of Ω_0^0 in the power expansion of the master equation (see appendix A) we obtain a

linear Fokker-Planck equation (see appendix B). This approximation is called as linear noise approximation[25] and the solution of the linear Fokker-Planck equation in appendix A is a Gaussian,[25] which means that the probability distribution $\Pi_t(\underline{\xi})$ is completely specified by the first two moments, $\langle \xi_\alpha(t) \rangle$ and $\langle \xi_\alpha^2(t) \rangle$, where $\alpha = S_j, I_j, L_j, \Phi$.

Multiplying the Fokker-Planck equation by ξ_α and $\xi_\alpha \xi_{\alpha'}$ and integrating over all $\underline{\xi}$ we find the time-evolution of the first and the second moments of noise, $\langle \xi_\alpha \rangle$ and $\langle \xi_\alpha \xi_{\alpha'} \rangle$ (see appendix B). The solutions of all first moments are simple: $\langle \xi_\alpha(t) \rangle = 0$ for all t, provided that the initial condition is chosen such that initial fluctuations vanish, i.e., $\langle \xi_\alpha(0) \rangle = 0$. The differential equations governing the time evolution of the second moments are coupled, and their solutions can only be attained by means of numerical integrations. We use the time evolution of the second moments of noise to study the role of stochastic fluctuations on phage-mediated competition, and especially to investigate the effects of noise on the invasion criterion. Let δN_j be the deviation of the total population size N_j of the jth bacterial strain from its average value, i.e., $\delta N_j = N_j - \langle N_j \rangle = \Omega_0^{1/2}(\xi_{S_j} + \xi_{I_j} + \xi_{L_j})$ where $N_j = S_j + I_j + L_j$ and $\langle N_j \rangle = \langle S_j \rangle + \langle I_j \rangle + \langle L_j \rangle$. Let us define the normalized variance of the total population size of the jth bacterial strain

$$Var(N_j) \equiv \frac{\langle \delta N_j^2 \rangle}{\langle N_j \rangle^2} = \frac{\Omega_0}{\langle N_j \rangle^2} \left\{ \left\langle \xi_{S_j}^2 \right\rangle + \left\langle \xi_{I_j}^2 \right\rangle + \left\langle \xi_{L_j}^2 \right\rangle + 2(\langle \xi_{S_j} \xi_{I_j} \rangle + \langle \xi_{S_j} \xi_{L_j} \rangle + \langle \xi_{I_j} \xi_{L_j} \rangle) \right\} \tag{7}$$

where $\langle . \rangle$ is a statistical ensemble average. The square root of the normalized variance, $\sqrt{\langle \delta N_j^2(t) \rangle} / \langle N_j(t) \rangle$, is the magnitude of noise of the jth bacterial strain at a given time t. Another useful quantity is the normalized co-variance between the ith bacterial strain in a state α and the jth bacterial strain in a state β:

$$Cov(\alpha_i, \beta_j) \equiv \frac{\langle \delta \alpha_i \delta \beta_j \rangle}{\langle N_i \rangle \langle N_j \rangle} = \frac{\Omega_0 \langle \xi_{\alpha_i} \xi_{\beta_j} \rangle}{\langle N_i \rangle \langle N_j \rangle} \tag{8}$$

We will present the results for these variances and co-variances in Sec. 5.

4. THE GILLESPIE ALGORITHM FOR STOCHASTIC SIMULATIONS

In this section we briefly describe our application of the Gillespie algorithm[27] for simulation of the stochastic process captured in the master equation of Eq. (2), where in total 12 biochemical reactions take place stochastically. The Gillespie algorithm consists of the iteration of the following steps: (i) selection of a waiting time τ during which no reaction occurs,

$$\tau = -\frac{1}{\sum_j a_j} ln\theta \tag{9}$$

where θ is a random variable uniformly chosen from an interval (0, 1) and a_j is the reaction rate for the jth biochemical reaction. (ii) After such a waiting time, which biochemical reaction will take place is determined by the following algorithm. The occurrence of each event has a weight $a_j / \sum_j a_j$. Thus the ith biochemical reaction is chosen if $\sum_{j=1}^{i} a_j < \theta' \sum_{j=1}^{N} a_j < \sum_{j=1}^{i+1} a_j$ where θ' is another random number selected from the interval (0, 1) and N is the total number of biochemical reactions. (iii) After execution of the jth reaction, all reaction rates that are affected by the jth reaction are updated.

We measure the averages, the normalized variances and co-variances of bacterial populations at various time points, by taking an average over 10^4 realizations of the infection process, starting with the same initial condition. Because a normalized variance or covariance is a measure of deviations of a stochastic variable from a macroscopic value (which is regarded as a true value), it is not divided by the sampling size.

The computing time of the Gillespie algorithm-based simulations increases exponentially with the system size. In the absence of resource competition, the total bacterial population increases exponentially in time. Because we need to know the stationary ratio of the two bacterial populations, the computing time should be long enough compared to typical time scales of the infection process. This condition imposes a limit on the range of parameters that we can explore to investigate the validity of the invasion criterion. We choose the values of parameters from the biologically relevant range given in Table II and we, furthermore, set lower bounds on the rates of infection causing contact κ_j and infection-induced lysis λ, namely $\kappa_j > \kappa_0$ and $\lambda > \lambda_0$.

5. RESULTS

While the methodologies described in Sec. 3 and 4 apply to the general case of two susceptible bacterial strains, in this section we limit our investigations to a particular infection system, called a "complete infection system" hereafter, in which bacterial strain 1 is completely lysogenic and only bacterial strain 2 is susceptible to phage infection. There are two advantages to studying the complete infection system: 1) this is equivalent to the infection system which we studied experimentally[21] and thus the results are immediately applicable to at least one real biological system. 2) the probabilistic description of bacterial strain 1 (lysogens) is analytically solvable as it corresponds to a stochastic birth-death process.[25] In Sec. 5.1, studying a system consisting of only lysogens, we elucidate the different dynamic patterns of the normalized variance when the system size remains constant or when it increases. This finding provides us with the asymptotic behavior of the normalized variances of both bacterial strains because both strains become lysogens eventually after all susceptible bacteria are depleted from the

system. In Sec. 5.2, we investigate the role of stochastic noise on phage-mediated competition by identifying the source of noise and assessing its magnitude in the complete infection system. Finally in Sec. 5.3, we investigate the effect of noise on the invasion criterion by means of stochastic simulations.

5.1. Stochastic Birth-Death Process: Growth and Spontaneous Lysis of Bacterial Strain 1

The dynamics of lysogens of bacterial strain 1 is completely decoupled from that of the rest of the complete infection system and can be studied independently. They grow at a rate r and are lysed at a rate δ. There exists an exact solution for the master equation of this stochastic birth-death process.[28,29] Thus we can gauge the accuracy of an approximate method for the corresponding stochastic process by comparing it with the exact solution. The master equation of the birth-death process is

$$\frac{dP_t(I_1)}{dt} = \left(E_{I_1}^{-1} - 1\right) r I_1 P_t(I_1) + \left(E_{I_1}^{+1} - 1\right) \delta I_1 P_t(I_1) \tag{10}$$

where $I_1(t)$ represents the number of lysogens at time t. I_1 is transformed into a new variable ξ_{I_1} as discussed in Sec. 3, which results in $I_1 = \Omega_0 i_1 + \Omega_0^{1/2}\xi_{I_1}$, $P_t(I_1) = \Pi_t(\xi_{I_1})$, and $E_{I_1}^{\pm 1} = 1 \pm \Omega_0^{-1/2}\frac{\partial}{\partial \xi_{I_1}} + \frac{\Omega_0^{-1}}{2}\frac{\partial^2}{\partial \xi_{I_1}^2}$. Then keeping terms of order Ω_0^0 from Ω_0-expansion of Eq. (10), we obtain the linear Fokker-Planck equation,

$$\frac{\partial \Pi_t(\xi_{I_1})}{\partial t} = (r+\delta)\frac{i_1}{2}\frac{\partial^2 \Pi_t(\xi_{I_1})}{\partial \xi_{I_1}^2} + (\delta - r)\frac{\partial \xi_{I_1}\Pi_t(\xi_{I_1})}{\partial \xi_{I_1}} \tag{11}$$

where $i_1(t) = I_1(t)/\Omega_o$ is a normalized quantity that evolves according to $\frac{di_1(t)}{dt} = (r-\delta)i_1(t)$ and $\Omega_0 = I_1(0)$. Multiplying by ξ_{I_1} and $\xi_{I_1}^2$ both sides of Eq. (11) and integrating over ξ_{I_1}, we obtain the equations for the first and the second moments of noise ξ_{I_1}:

$$\begin{aligned} \frac{d\langle \xi_{I_1}\rangle}{dt} &= (r-\delta)\langle \xi_{I_1}\rangle \\ \frac{d\langle \xi_{I_1}^2\rangle}{dt} &= (r+\delta)i_1 + 2(r-\delta)\langle \xi_{I_1}^2\rangle \end{aligned} \tag{12}$$

Case 1. $r > \delta$. When the growth rate is greater than the lysis rate, the system size is increasing in time and the second moment of ξ_{I_1} evolves in time according to the solution of Eq. (12): $\langle \xi_{I_1}^2(t)\rangle = \frac{(r+\delta)}{(r-\delta)} i_1(0) e^{2(r-\delta)t}(1 - e^{-(r-\delta)t})$. Then the normalized variance of lysogens reads

$$\frac{\langle \delta I_1^2(t)\rangle}{\langle I_1(t)\rangle^2} = \frac{\Omega_0 \langle \xi_{I_1}^2(t)\rangle}{\langle I_1(t)\rangle^2} = \frac{(r+\delta)}{(r-\delta)I_1(0)}(1 - e^{-(r-\delta)t}) \tag{13}$$

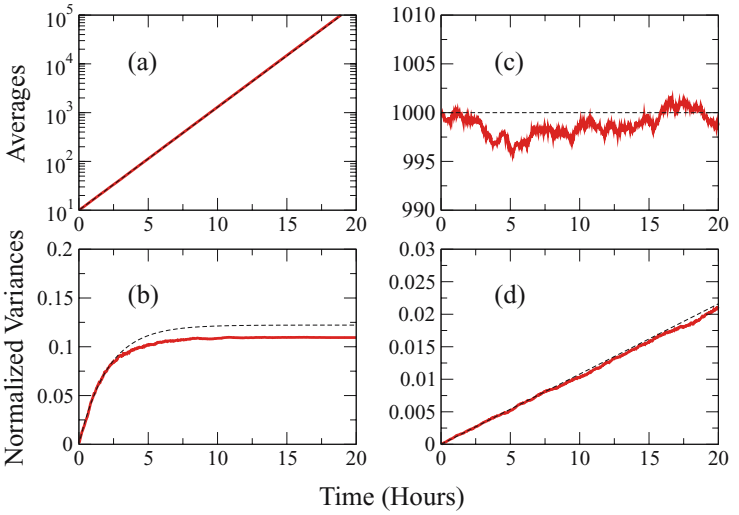

Fig. 4. (Color online) Time-evolution of the normalized variance of a birth-death process of lysogens when the system size increases (a, b), or when it remains constant (c, d). (a, b) are time-evolutions of the mean and the normalized variance of lysogens when the system size increases exponentially in time, $r = 0.54$ and $\delta = 0.054$. (c, d) depict those of lysogens when their growth and lysis rates are the same, $r = \delta = 0.54$. Solid lines represent the results of stochastic simulations while dotted lines are the results of the macroscopic equation (a, c) or the results of the linear Fokker-Planck equation (b, d).

Asymptotically the normalized variance approaches a constant value $(r + \delta)/((r - \delta)I_1(0))$, in good agreement with the results of stochastic simulations (see Fig. 4(b)).

Case 2. $r = \delta$. When the growth rate is the same as the lysis rate, the system size remains constant and the normalized variance increases linearly in time: $\langle \delta I_1^2(t) \rangle / \langle I_1(t) \rangle^2 = (r + \delta)t/I_1(0)$, exactly reproduced by stochastic simulations as shown in Fig. 4(d).

5.2. Complete Infection System: The Dynamics of Covariances of Stochastic Fluctuations

In this subsection, we discuss the effects of noise on phage-mediated competition. We explore the dynamical patterns of the normalized variances and covariances of the complete infection system, from which we identify the major source of stochastic fluctuations and assess their magnitude. In the complete infection system, all bacteria in strain 1 are lysogens and all bacteria in strain 2 are susceptible to phage infection. Bacterial strain 1 (lysogens), while decoupled from the rest of the system, play a role as the source of the phage, triggering a massive

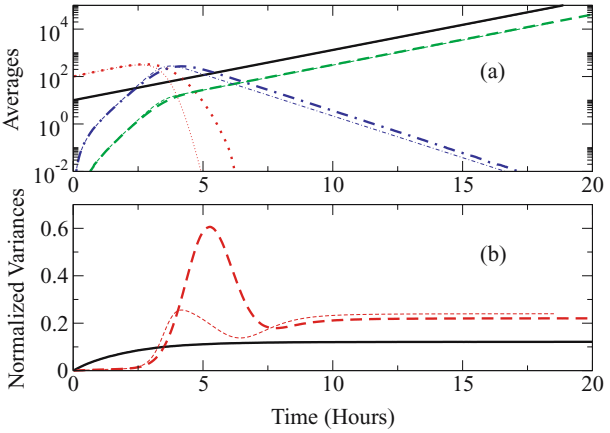

Fig. 5. (Color online) Time-evolution of the mean values of bacterial subpopulations (a) and the normalized variance of total population of bacterial strain 1 and 2 (b). (a) Each subpopulation is represented by two lines; thick lines come from macroscopic equations in Eq (5) and thin lines are obtained from stochastic simulations. The four bacterial subpopulations are represented by different line patterns: bacterial strain 1 in lysogenic state (solid lines), bacterial strain 2 in susceptible (dotted lines), lysogenic (dashed lines) and latent (dot-dashed lines) states. (b) Thick solid and dashed lines represent the normalized variances of the bacterial strain 1 and 2 from stochastic simulations, respectively, while thin solid and dashed lines denote those from the linear Fokker-Planck equation, respectively. The initial condition is $I_1(0) = 10$, $S_2(0) = 100$ and the rest are zero. The parameter values are $\delta = 0.054$, $\lambda = 0.81$, $\kappa_2 = 0.00054$, $\chi = 50$, and $P_2 = 0.98$.

infection process in the susceptible bacterial strain 2. Throughout this subsection, we make pair-wise comparisons between the results of the deterministic equations, stochastic simulations and of the linear Fokker-Planck equation.

Figure 5(a) shows the time evolution of bacterial populations in the susceptible, lysogenic and latent states. While bacteria of strain 1 (lysogens) grow exponentially unaffected by phage, the susceptible bacteria of strain 2 undergo a rapid infection process, being converted either into a latent state or into lysogens. The number of bacteria in the latent state increases, reaches a peak at a later stage of infection process, and then decays exponentially at a rate λ. As time elapses, eventually all susceptible bacteria are depleted from the system and both bacterial strains become lysogens, which grow at a net growth rate $a - \delta$. The ratio of the two bacterial strains (lysogens) remains unchanged asymptotically. Note that although the initial population size of bacterial strain 1 is one-tenth of the initial population size of bacterial strain 2, strain 1 will outnumber strain 2 at a later time due to phage-mediated competition. Pair-wise comparisons between the results from stochastic simulation and those from deterministic equations are made in Fig.5(a). They agree nicely with each other except a noticeable discrepancy found in the population size of susceptible bacteria.

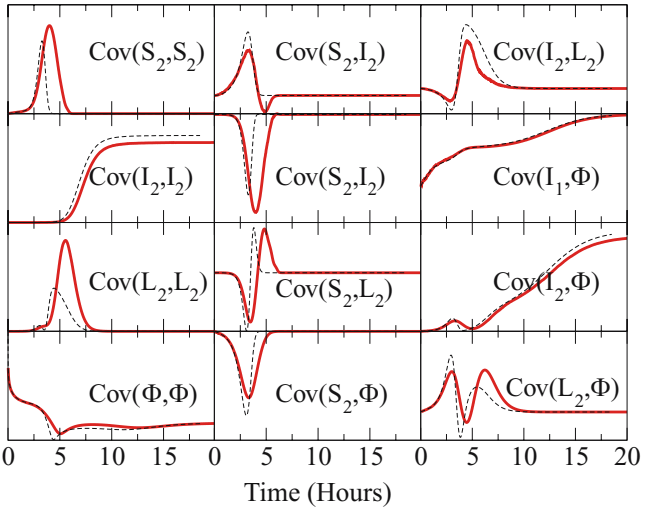

Fig. 6. (Color online) Time evolution of the normalized (co-)variances of bacterial populations in different states. See the main text for a formal definition of the normalized covariance $\mathrm{Cov}(\alpha_i, \beta_j)$. The time-evolution of each co-variance is plotted with two lines: solid lines are from stochastic simulations while dashed lines are from the linear Fokker-Planck equation. The same parameters and initial conditions are used as in Fig. 5. Only 12 out of 15 co-variances are plotted.

The temporal patterns of the normalized variances of the two bacterial strains are illustrated in Fig. 5(b). The normalized variance of bacterial strain 1 (lysogens) increases logistically while that of bacterial strain 2 increases logistically for the first few hours and then rapidly rises to its peak upon the onset of a massive phage infection process taking place in the susceptible bacterial strain 2. Asymptotically, susceptible bacteria are depleted from the system and all remaining bacteria are lysogens, and their normalized variances converge to a constant as given by Eq. (13). Note that the linear Fokker-Planck equation underestimates the peak value of the normalized variance, compared to the stochastic simulations, while the stationary values of the normalized variances of both bacterial strains from two methods agree nicely. The temporal behavior of the normalized variance of the bacterial strain 2, i.e., the fact that it first peaks and then reaches a plateau, implies two different sources of noise at two different time limits.

We use the dynamical patterns of the normalized covariances shown in Fig. 6 to identify the source of stochastic fluctuations in phage-mediated competition. The normalized variance of the total population of bacterial strain 2, $Var(N_2)$, is composed of the 6 normalized covariances of the subpopulations of bacterial strain 2, $Cov(S_2, S_2)$, $Cov(I_2, I_2)$, $Cov(L_2, L_2)$, $Cov(S_2, I_2)$, $Cov(S_2, L_2)$ and $Cov(I_2, L_2)$, among which the peak values of $Cov(S_2, S_2)$, $Cov(I_2, I_2)$ and $\mathrm{Cov}(L_2, L_2)$ are 10 times as large as those of $\mathrm{Cov}(S_2, I_2)$, $Cov(S_2, L_2)$ and

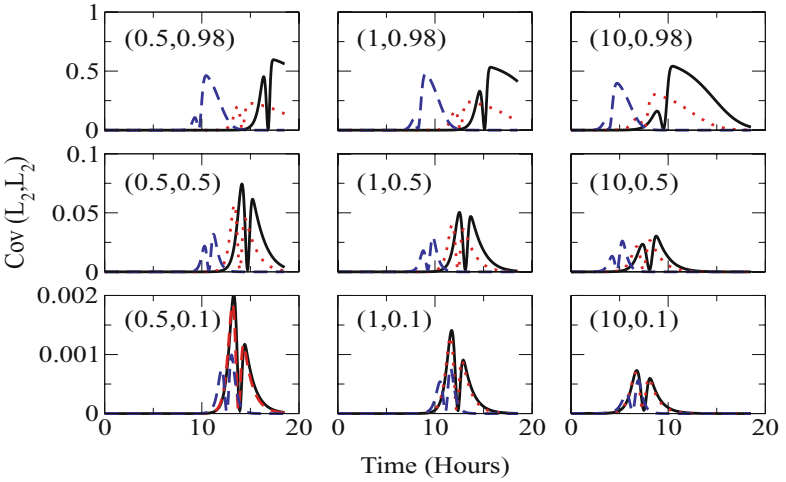

Fig. 7. (Color online) Time-evolution of the normalized covariance of the latent population of the bacterial strain 2, Cov(L_2, L_2), as a function of the phage pathology, the contact rate κ, and the infection-induced lysis rate λ. These time-evolutions are obtained by numerically solving the second moment equations derived from the linear Fokker-Planck equation. A set of different values of κ and P, (κ, P), is assigned to each panel. Each panel contains three different time-evolutions with three different values of λ: 0.5 for the solid line, 1 for the dotted line and 10 for the dashed line. The initial conditions and the other parameter values are the same as in Fig. 5.

$Cov(I_2, L_2)$ for this particular choice of parameters. At the earlier time when the phage infection takes place actively, the normalized covariance of the latent population, $Cov(L_2, L_2)$, reaches its peak value, the largest value among all normalized covariances, at the exact moment when the normalized variance of the total population of the bacterial strain 2, $Var(N_2)$, hits its maximum value. Thus the peak of the normalized variance of the total population of the bacterial strain 2 in Fig. 5(b) comes from the stochastic fluctuations of the bacterial population in the latent state. At the later time when no infection takes place anymore, the stationary normalized variance of the total population of the bacterial strain 2 originates solely from the stochastic fluctuations of the bacterial population in the lysogenic state, represented by $Cov(I_2, I_2)$. Both Cov(L_2, L_2) and $Cov(I_2, I_2)$ ultimately affect the stationary ratio of two bacterial populations in the presence of noise.

The magnitude of the stochastic fluctuations of the initially susceptible bacterial population is determined predominantly by the phage pathology value. We evaluated the peak value of the normalized covariance of the latent population, Cov(L_2, L_2), and the stationary value of the normalized covariance of the lysogenic population, Cov(I_2, I_2), by using both the Fokker-Planck equation and stochastic simulations, with different values of phage pathology, infection-causing contact

rate and the infection induced lysis rate (see Fig. 7). Both values depend mainly on the phage pathology and increase as the phage pathology value increases to 1. For the peak value of $\mathrm{Cov}(L_2, L_2)$, when P increases to 1, the average total population size of the bacterial strain 2, i.e., the denominator of $\mathrm{Cov}(L_2, L_2)$, decreases and consequently the peak value of $\mathrm{Cov}(L_2, L_2)$ increases. For the stationary value of $\mathrm{Cov}(I_2, I_2)$, as P increases, the average population size of lysogens at the moment when all susceptible bacteria are depleted increases and the stationary value of $\mathrm{Cov}(I_2, I_2)$ increases according to Eq. (13) where the average size of lysogens at this moment is used as $I_1(0)$.

As shown in Fig. 6, the time evolutions of the normalized covariances obtained from the stochastic simulations are correctly captured by the linear Fokker-Planck equation. Considering that the latter represents a linear approximation of the master equation of the present nonlinear dynamical system, the agreement between the temporal patterns from two methods is impressive. There are several obvious disagreements between the results obtained from the two methods. The peak value of the covariance of the latent population obtained by stochastic simulations is twice as large as that by Fokker-Planck equation, and the temporal profiles of the covariances from the Fokker-Planck equation are slightly shifted to the left, compared to those obtained by stochastic simulations. The discrepancies could be due to the nonlinear fluctuations affected by the presence of nonlinear terms in the macroscopic equation in Eq. (5) and necessitate us to go beyond the linear noise approximation. A second order Fokker-Planck equation can be obtained by identifying terms of $\Omega_0^{-1/2}$ in the power expansion of the master equation (see Appendix A). As a result, one can obtain the closed system of second, third and fourth moment equations of noise. This is, however, impractical for the present bacteria-phage system because the number of the moment equations for the higher order Fokker-Planck equation grows exponentially, e.g., there are more than 300 moment equations for the second order Fokker-Planck equation.

5.3. The Effect of Stochastic Noise on the Invasion Criterion

In this subsection we investigate the effects of noise on the validity of the invasion criterion and measure the deviations of the stochastic results from the simple relationship in Eq. (6) obtained from the deterministic model. For further analysis of the effect of noise on phage-mediated competition, we need to perform stochastic simulations with different values of kinetic parameters and to investigate the effect of noise on the invasion criterion. We consider both a complete infection system having only lysogens in bacterial strain 1 ($P_1 = 0$) in Fig. 8(a) and a generalized infection system in Fig. 8(b) where both strains are susceptible to phage infection, yet with different degrees of susceptibility and vulnerability to phage. The invasion criterion obtained from the deterministic equations is expressed with

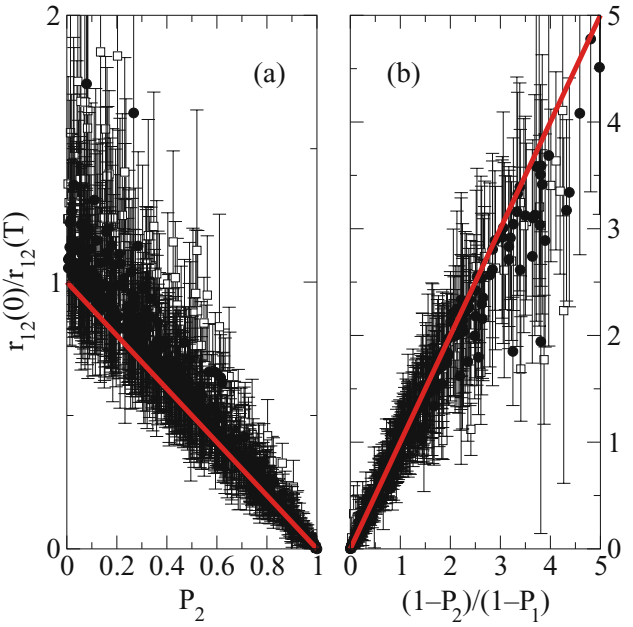

Fig. 8. (Color online) Verification of the invasion criterion by means of stochastic simulations: (a) a complete infection system case where bacterial strain 1 is lysogen and only bacterial strain 2 is susceptible, (b) a general infection system where both strains are susceptible to phage. Thick red lines represent the invasion criterion obtained from deterministic equations, i.e., $r_{12}(0)/r_{12}(T) = (1 - P_2)/(1 - P_1)$ where the time T is chosen to be a sufficiently long time so that there are no more susceptible bacteria in the system. Error bars are the standard deviations calculated from the stochastic simulation. Filled circles are for a fast infection process ($\kappa > 10\kappa_o$,$\lambda > 10\lambda_o$) while open squares are for slow infection ($\kappa_o < \kappa < 10\kappa_o$,$\lambda_o < \lambda < 10\lambda_o$). Each one of about 500 data points in each figure represents the result of stochastic simulations, averaged over 10^4 realizations. Please see the main text for the choice of parameter values.

a simple relationship between the initial and final ratios of population sizes of two strains and phage pathologies: $r_{12}(0)/r_{12}(T) = (1 - P_2)/(1 - P_1)$. Here T is defined as a sufficiently long time such that there are no more susceptible bacteria left to undergo the infection process and only lysogens are in the system. To amplify the effect of noise on phage-mediated competition, we set the initial sizes of bacterial populations to be small; they are randomly chosen from an interval $10 < S_j(0), I_j(0) < 110$. To make sure that the complete infection system reaches a stationary state of having only lysogens within 24 hours, we limit the values of the infection-causing contact rate κ_j and of the infection-induced lysis rate λ: $\kappa_j > \kappa_o$ and $\lambda > \lambda_o$ where $\kappa_o = 0.000054$ and $\lambda_o = 0.081$. We distinguish infection processes based on their speed: a very fast infection process ($\kappa > 10\kappa_o$, $\lambda > 10\lambda_o$) and a slow infection process ($\kappa_o < \kappa < 10\kappa_o$, $\lambda_o < \lambda < 10\lambda_o$). The

values of all other kinetic parameters in Fig. 2 are randomly selected from the biologically relevant intervals (see Table 1): $0 < \delta < 0.108$, $1 < \chi < 100$ and $0 < P_j < 1$. For about 500 sets of parameters for each figure in Fig. 8, we measure the average and the standard deviation of the stationary ratio $r_{12}(0)/r_{12}(T)$ after taking ensemble average over 10^4 realizations. Note that the standard deviation is measured as a deviation from the macroscopic (true) value and it is not normalized by the square root of the sampling size. We find that the average values of the stationary ratios $r_{12}(0)/r_{12}(T)$ still fall onto the linear relationship with phage pathologies, independently of other kinetic parameters.

As depicted in Fig. 8, the magnitude of the stochastic fluctuations in the stationary ratio of two bacterial population sizes, $r_{12}(0)/r_{12}(T)$, is determined predominantly by the phage pathology value, independently of other kinetic parameters of the system. For the complete infection system in Fig. 8(a), the standard deviation of the stationary ratio increases when the phage pathology P_2 decreases, and for the general infection system in Fig. 8(b), where both strains are susceptible to phage infection, the standard deviation of the stationary ratio increases when the phage is more pathological to bacterial strain 1 than to bacterial strain 2. For the case of the complete infection system in Fig. 8(a), the standard deviation of the stationary ratio is approximately proportional to the standard deviation of the total population size of bacterial strain 2, which is proportional to the square root of the total population size of bacterial strain 2. As P_2 decreases, the total population size of bacterial strain 2 at a fixed large time T increases, and thus the standard deviation of the stationary ratio increases. For the case of the general infection system in Fig. 8(b), the standard deviation of the stationary ratio is approximately proportional to the ratio of the standard deviation of the total population size of bacterial strain 2 to the average population size of bacterial strain 1. As the difference between the phage pathology on bacterial strain 1 (P_1) and on bacterial strain 2 (P_2), i.e., $P_1 - P_2$, increases, the average population size of bacterial strain 1 decreases (when P_1 increases) or the standard deviation of the total population size of bacterial strain 2 increases (when P_2 decreases). As a result the standard deviation of the stationary ratio of two bacterial population sizes increases. Thus we used the probabilistic model of phage-mediated competition in bacteria to show that the phage pathology value determines not only the average amount but also the magnitude of noise of phage-mediated competition, i.e., the invasion criterion as illustrated in Eq. (6).

6. CONCLUSION

We utilized a probabilistic model of a phage-mediated invasion process to investigate the conjecture that (i) a bacterial community structure is shaped by phage-mediated competition between bacteria, and to examine (ii) the effect of intrinsic noise on the conclusions obtained from a deterministic model of the

equivalent system. We consider a generalized phage infection system where two bacterial strains are susceptible to phage infection, yet with different degrees of susceptibility and vulnerability to phage.

Despite the historical success of deterministic models of ecological processes, they produce, at best, only partially correct pictures of stochastic processes in ecological systems. A good number of examples of the failures of deterministic models in ecology are presented in Ref. 2. The principal flaw of deterministic models is their reliance on many, sometimes unphysical, assumptions such as continuous variables, complete mixing and no rare events. Thus, we used both Fokker-Planck equations and stochastic simulations in the study of stochastic phage-mediated invasion processes in bacteria. Van Kampen's system size expansion[25] was used to obtain the linear Fokker-Planck equation while the Gillespie algorithm was used for stochastic simulations. We found that the linear Fokker-Planck equation is a good approximation to the nonlinear dynamics of the stochastic phage-mediated invasion process; the time evolutions of co-variances of bacterial populations from both Fokker-Planck equation and stochastic simulations agree well with each other.

To understand the role of noise during phage-mediated processes, we defined noise as the ratio of the standard deviation of a bacterial population to its mean size, identified its source, and measured its magnitude. Both analytical and numerical analysis of the probabilistic model of the phage-mediated competition showed that the initial transient noise originates from the stochastic fluctuations in the latent bacterial population while the stationary noise is determined by fluctuations in the lysogenic bacterial population. The magnitude of the noise is determined predominantly by the phage pathology value, independently of other kinetic parameters: as the phage pathology increases, the magnitude of the noise, measured as the normalized covariance, increases.

We investigated the effect of noise on the invasion criterion, which is defined as the condition of the system parameters for which the invading bacterial strain 1 outnumbers the resident bacterial strain 2. We found from stochastic simulations that both the average values and the standard deviations of the stationary ratios $r_{12}(0)/r_{12}(T)$ are solely determined by the phage pathology, independently of other kinetic parameters. The standard deviation of the stationary ratio increases as the difference between the phage pathology on bacterial strain 1 and on bacterial strain 2, i.e., $P_1 - P_2$, increases. Thus the probabilistic model of phage-mediated competition in bacteria confirms that the quantitative amount of phage-mediated competition as well as the deviations from the deterministic invasion criterion (Eq. (6)) can still be predictable despite inherent stochastic fluctuations.

Here we assumed that the bacterial growth rates and lysis rates are identical in the two strains. Relaxing this assumption has a drastic simplifying effect as the steady state is determined solely by the net growth rates of the two strains. Regardless of initial conditions in the generalized infection system, all bacteria that survive after a massive phage infection process are lysogens, so long as the

phage-infection is in action on both bacterial strains. If the net growth rates of two strains are such that $r_1 - \delta_1 > r_2 - \delta_2 > 0$, asymptotically bacterial strain 1 will outnumber strain 2, regardless of phage pathologies and initial population sizes. If the net growth rate of any bacterial strain is negative, it will go extinct. Thus the non-trivial case is only when the growth rates of two bacterial strains are identical.

We significantly simplified many aspects of complex pathogen-mediated dynamical systems to obtain this stochastic model. The two most prominent yet neglected features are the spatial distribution and the connectivity pattern of the host population. As demonstrated by stochastic contact processes on complex networks (e.g., infinite scale-free networks) or on d-dimensional hypercubic lattices,[3,3,30–33] these two effects may dramatically change the dynamics and stationary states of the pathogen-mediated dynamical systems. While our experimental system does not necessitate incorporation of spatial effects, complete models of real pathogen-modulated ecological processes, e.g., phage-mediated competition as a driving force of the oscillation of two V. cholera bacterial strains, one toxic (phage-sensitive) and the other non-toxic (phage-carrying and resistant), [34] may need to take these effects into account.

APPENDIX A: SYSTEMATIC EXPANSION OF THE MASTER EQUATION

In this appendix we provide the result of the systematic expansion of the master equation in Eq. (2). The master equation in the new variables reads

$$
\begin{aligned}
&\frac{\partial \Pi}{\partial t} - \sum_{\alpha=S_1,S_2,I_1,I_2,L_1,L_2,\Phi} \left\{ \Omega_0^{\frac{1}{2}} \frac{\partial \alpha}{dt} \frac{\partial \Pi}{\partial \xi_\alpha} \right\} \\
&= \sum_j \left\{ a \sum_{\alpha=S_j,I_j} \left\{ \left(-\Omega_0^{-\frac{1}{2}} \frac{\partial}{\partial \xi_\alpha} + \frac{\Omega_0^{-1}}{2} \frac{\partial^2}{\partial \xi_\alpha^2} - \cdots \right) \left(\Omega_0 \alpha + \Omega_0^{\frac{1}{2}} \xi_\alpha \right) \Pi \right\} \right. \\
&+ \kappa_j \left\{ \left(1 + \Omega_0^{-\frac{1}{2}} \frac{\partial}{\partial \xi_\Phi} + \frac{\Omega_0^{-1}}{2} \frac{\partial^2}{\partial \xi_\Phi^2} + \cdots \right) \left(1 + \Omega_0^{-\frac{1}{2}} \frac{\partial}{\partial \xi_{S_j}} + \frac{\Omega_0^{-1}}{2} \frac{\partial^2}{\partial \xi_{S_j}^2} + \cdots \right) \right. \\
&\quad \times \left[(1 - P_j) \left(1 - \Omega_0^{-\frac{1}{2}} \frac{\partial}{\partial \xi_{I_j}} + \frac{\Omega_0^{-1}}{2} \frac{\partial^2}{\partial \xi_{I_j}^2} - \cdots \right) \right. \\
&\left. \left. \left. + P_j \left(1 - \Omega_0^{-\frac{1}{2}} \frac{\partial}{\partial \xi_{L_j}} + \frac{\Omega_0^{-1}}{2} \frac{\partial^2}{\partial \xi_{L_j}^2} - \cdots \right) \right] - 1 \right\} \right. \\
&\quad \times \left(\Omega_0 \phi + \Omega_0^{\frac{1}{2}} \xi_\Phi \right) \left(\Omega_0 s_j + \Omega_0^{\frac{1}{2}} \xi_{S_j} \right) \Pi
\end{aligned}
$$

$$
\begin{aligned}
&+\delta\Bigg\{\left(1+\Omega_0^{-\frac{1}{2}}\frac{\partial}{\partial\xi_{I_j}}+\frac{\Omega_0^{-1}}{2}\frac{\partial^2}{\partial\xi_{I_j}^2}+\cdots\right)\\
&\quad\times\left(1-\Omega_0^{-\frac{1}{2}}\frac{\partial}{\partial\xi_{\Phi}}+\frac{\Omega_0^{-1}}{2}\frac{\partial^2}{\partial\xi_{\Phi}^2}+\cdots\right)^{\chi}-1\Bigg\}\left(\Omega_0 i_j+\Omega_0^{\frac{1}{2}}\xi_{I_j}\right)\Pi\\
&+\lambda\Bigg\{\left(1+\Omega_0^{-\frac{1}{2}}\frac{\partial}{\partial\xi_{L_j}}+\frac{\Omega_0^{-1}}{2}\frac{\partial^2}{\partial\xi_{L_j}^2}+\cdots\right)\\
&\left(1-\Omega_0^{-\frac{1}{2}}\frac{\partial}{\partial\xi_{\Phi}}+\frac{\Omega_0^{-1}}{2}\frac{\partial^2}{\partial\xi_{\Phi}^2}+\cdots\right)^{\chi}-1\Bigg\}\\
&\times\left(\Omega_0 l_j+\Omega_0^{\frac{1}{2}}\xi_{L_j}\right)\Pi\Bigg\}
\end{aligned}
\tag{14}
$$

APPENDIX B: LINEAR FOKKER-PLANCK EQUATION DERIVED FROM SYSTEMATIC EXPANSION OF THE MASTER EQUATION

From Eq. (14) we can collect terms of order Ω^0 and obtain the linear Fokker Planck equation,

$$
\begin{aligned}
\frac{\partial\Pi}{\partial t}=\sum_j\Bigg\{&a\Bigg(-\frac{\partial\xi_{S_j}\Pi}{\partial\xi_{S_j}}-\frac{\partial\xi_{I_j}\Pi}{\partial\xi_{I_j}}+\frac{s_j}{2}\frac{\partial\Pi}{\partial\xi_{S_j}^2}+\frac{i_j}{2}\frac{\partial\Pi}{\partial\xi_{I_j}^2}\Bigg)\\
&+\kappa_j\Omega_0\phi s_j\Bigg\{\frac{\partial^2}{\partial\xi_{\Phi}\partial\xi_{S_j}}+\frac{1}{2}\left(\frac{\partial^2}{\partial\xi_{\Phi}^2}+\frac{\partial^2}{\partial\xi_{S_j}^2}\right)+(1-P_j)\\
&\quad\times\left(\frac{1}{2}\frac{\partial^2}{\partial\xi_{I_j}^2}-\frac{\partial^2}{\partial\xi_{\Phi}\partial\xi_{I_j}}-\frac{\partial^2}{\partial\xi_{S_j}\partial\xi_{I_j}}\right)\\
&+P_j\left(\frac{1}{2}\frac{\partial^2}{\partial\xi_{L_j}^2}-\frac{\partial^2}{\partial\xi_{\Phi}\partial\xi_{L_j}}-\frac{\partial^2}{\partial\xi_{S_j}\partial\xi_{L_j}}\right)\Bigg\}\Pi+\kappa_j\Omega_0\\
&\left\{\frac{\partial}{\partial\xi_{\Phi}}+\frac{\partial}{\partial\xi_{S_j}}-(1-P_j)\frac{\partial}{\partial\xi_{I_j}}-P_j\frac{\partial}{\partial\xi_{L_j}}\right\}(\phi\xi_{S_j}\Pi+s_j\xi_{\Phi}\Pi)\\
&+\delta\left\{\frac{\partial\xi_{I_j}\Pi}{\partial\xi_{I_j}}-\chi\frac{\partial\xi_{I_j}\Pi}{\partial\xi_{\Phi}}+\frac{i_j}{2}\frac{\partial^2\Pi}{\partial\xi_{I_j}^2}+i_j\frac{\chi^2}{2}\frac{\partial^2\Pi}{\partial\xi_{\Phi}^2}-\chi i_j\frac{\partial^2\Pi}{\partial\xi_{I_j}\partial\xi_{\Phi}}\right\}
\end{aligned}
$$

$$+\lambda\left\{\frac{\partial\xi_{L_j}\Pi}{\partial\xi_{L_j}}-\chi\frac{\partial\xi_{L_j}\Pi}{\partial\xi_\Phi}+\frac{l_j}{2}\frac{\partial^2\Pi}{\partial\xi_{L_j}^2}+l_j\frac{\chi^2}{2}\frac{\partial^2\Pi}{\partial\xi_\Phi^2}-\chi l_j\frac{\partial^2\Pi}{\partial\xi_{L_j}\partial\xi_\Phi}\right\}\Bigg\} \tag{15}$$

We obtain the first moments of the Gaussian noise by multiplying the Eq. (15) by ξ_α and integrating over all $\underline{\xi}$, i.e., $\int \xi_\alpha d\Pi = \langle\xi_\alpha\rangle$.

$$\begin{aligned}
\frac{d\langle\xi_{S_j}\rangle}{dt} &= a\langle\xi_{S_j}\rangle-\kappa_j\Omega_0(\phi\langle\xi_{S_j}\rangle+s_j\langle\xi_\Phi\rangle)\\
\frac{d\langle\xi_{I_j}\rangle}{dt} &= (a-\delta)\langle\xi_{I_j}\rangle+\kappa_j\Omega_0(1-P_j)(\phi\langle\xi_{S_j}\rangle+s_j\langle\xi_\Phi\rangle)\\
\frac{d\langle\xi_{L_j}\rangle}{dt} &= \kappa_j\Omega_0P_j(\phi\langle\xi_{S_j}\rangle+s_j\langle\xi_\Phi\rangle)-\lambda\langle\xi_{L_j}\rangle\\
\frac{d\langle\xi_\Phi\rangle}{dt} &= \sum_j\{\delta\chi\langle\xi_{I_j}\rangle+\lambda\chi\langle\xi_{L_j}\rangle-\kappa_j\Omega_0\phi(\langle\xi_{S_j}\rangle+s_j\langle\xi_\Phi\rangle)\}
\end{aligned} \tag{16}$$

Similarly we obtain the second moments (covariance) of the Gaussian noise by multiplying the Eq. (15) by $\xi_\alpha\xi_\beta$ and integrating over all $\underline{\xi}$, i.e., $\int \xi_\alpha\xi_\beta d\Pi = \langle\xi_\alpha\xi_\beta\rangle$.

$$\begin{aligned}
\frac{d\langle\xi_{S_j}\xi_{S_{j'}}\rangle}{dt} &= 2a\langle\xi_{S_j}\xi_{S_{j'}}\rangle+(as_j+\kappa_j\Omega_0s_j\phi)\delta_{jj'}\\
&\quad-\left\{\kappa_j\Omega_0(\langle\xi_{S_j}\xi_{S_{j'}}\rangle\phi+\langle\xi_{S_{j'}}\xi_\Phi\rangle s_j)+(j\leftrightarrow j')\right\}\\
\frac{d\langle\xi_{I_j}\xi_{I_{j'}}\rangle}{dt} &= 2a\langle\xi_{I_j}\xi_{I_{j'}}\rangle+(ai_j+\delta i_j+k_j\Omega_0\phi s_j(1-P_j))\delta_{jj'}-2\delta\langle\xi_{I_j}\xi_{I_{j'}}\rangle\\
&\quad+\left\{\kappa_j\Omega_0(1-P_j)(\langle\xi_{S_j}\xi_{I_{j'}}\rangle\phi+\langle\xi_{I_{j'}}\xi_\Phi\rangle s_j)+(j\leftrightarrow j')\right\}\\
\frac{d\langle\xi_{L_j}\xi_{L_{j'}}\rangle}{dt} &= (\lambda l_j+k_j\Omega_0\phi s_jP_j)\delta_{jj'}-2\lambda\langle\xi_{L_j}\xi_{L_{j'}}\rangle+\left\{\kappa_j\Omega_0P_j(\langle\xi_{S_j}\xi_{L_{j'}}\rangle\phi\right.\\
&\quad\left.+\langle\xi_{L_{j'}}\xi_\Phi\rangle s_j)+(j\leftrightarrow j')\right\}\\
\frac{d\langle\xi_\Phi^2\rangle}{dt} &= \sum_j\left\{\kappa_j\Omega_0s_j\phi-2\kappa_j\Omega_0(\langle\xi_{S_j}\xi_\Phi\rangle\phi+\langle\xi_\Phi^2\rangle s_j)+2\chi(\delta\langle\xi_{I_j}\xi_\Phi\rangle\right.\\
&\quad\left.+\lambda\langle\xi_{L_j}\xi_\Phi\rangle)+\chi^2(\delta i_j+\lambda l_j)\right\}\\
\frac{d\langle\xi_{S_j}\xi_{I_{j'}}\rangle}{dt} &= 2a\langle\xi_{S_j}\xi_{I_{j'}}\rangle-(1-P_j)\kappa_j\Omega_0s_j\phi\delta_{j,j'}-\kappa_j\Omega_0(\langle\xi_{S_j}\xi_{I_{j'}}\rangle\phi+\langle\xi_{I_{j'}}\xi_\Phi\rangle s_j)\\
&\quad+(1-P_{j'})\kappa_{j'}\Omega_0(\langle\xi_{S_j}\xi_{S_{j'}}\rangle\phi+\langle\xi_{S_j}\xi_\Phi\rangle s_{j'})-\delta\langle\xi_{S_j}\xi_{I_{j'}}\rangle
\end{aligned}$$

$$\frac{d\langle \xi_{S_j}\xi_{L_{j'}}\rangle}{dt} = a\langle \xi_{S_j}\xi_{L_{j'}}\rangle - P_j\kappa_j\Omega_0 s_j\phi\delta_{j,j'} - \lambda\langle \xi_{S_j}\xi_{L_{j'}}\rangle - \kappa_j\Omega_0(\langle \xi_{S_j}\xi_{L'_j}\rangle\phi + \langle \xi_{L_{j'}}\xi_\Phi\rangle s_j) + P_{j'}\kappa_{j'}\Omega_0(\langle \xi_{S_j}\xi_{S_{j'}}\rangle\phi + \langle \xi_{S_j}\xi_\Phi\rangle s_{j'}) \tag{17}$$

$$\begin{aligned}
\frac{d\langle \xi_{S_j}\xi_\Phi\rangle}{dt} &= a\langle \xi_{S_j}\xi_\Phi\rangle + \kappa_j\Omega_0 s_j\phi + \chi\sum_{j'}(\delta\langle \xi_{S_j}\xi_{I_{j'}}\rangle + \lambda\langle \xi_{S_j}\xi_{L_{j'}}\rangle) \\
&\quad - \sum_{j'}(\kappa_{j'}\Omega_0\langle \xi_{S_{j'}}\xi_{S_j}\rangle\phi + \kappa_{j'}\Omega_0\langle \xi_{S_j}\xi_\Phi\rangle s_{j'}) \\
&\quad -\kappa_j\Omega_0(\langle \xi_{S_j}\xi_\Phi\rangle\phi + \langle \xi_\Phi^2\rangle s_j) \\
\frac{d\langle \xi_{I_j}\xi_{L_{j'}}\rangle}{dt} &= (a-\delta)\langle \xi_{I_j}\xi_{L_{j'}}\rangle - \lambda\langle \xi_{I_j}\xi_{L_{j'}}\rangle + \kappa_j\Omega_0(1-P_j)(\langle \xi_{S_j}\xi_{L_{j'}}\rangle\phi \\
&\quad + \langle \xi_{L_{j'}}\xi_\Phi\rangle s_j) + \kappa_{j'}\Omega_0 P_{j'}(\langle \xi_{I_j}\xi_{S_{j'}}\rangle\phi + \langle \xi_{I_j}\xi_\Phi\rangle s_{j'}) \\
\frac{d\langle \xi_{I_j}\xi_\Phi\rangle}{dt} &= (a-\delta)\langle \xi_{I_j}\xi_\Phi\rangle - \delta\chi i_j + \chi\sum_{j'}(\lambda\langle \xi_{I_j}\xi_{L_{j'}}\rangle + \delta\langle \xi_{I_j}\xi_{I_{j'}}\rangle) \\
&\quad -\kappa_j\Omega_0 s_j\phi(1-P_j) - \sum_{j'}\kappa_{j'}\Omega_0(\langle \xi_{S_{j'}}\xi_{I_j}\rangle\phi + \langle \xi_{I_j}\xi_\Phi\rangle s_{j'}) \\
&\quad +\kappa_j\Omega_0(1-P_j)(\langle \xi_{S_j}\xi_\Phi\rangle\phi + \langle \xi_\Phi^2\rangle s_j) \\
\frac{d\langle \xi_{L_j}\xi_\Phi\rangle}{dt} &= -P_j\kappa_j\Omega_0 s_j\phi - \lambda\chi l_j - \lambda\langle \xi_\Phi\xi_{L_j}\rangle + \chi\sum_{j'}(\delta\langle \xi_{L_j}\xi_{I_{j'}}\rangle + \lambda\langle \xi_{L_j}\xi_{L_{j'}}\rangle) \\
&\quad - \sum_{j'}\kappa_{j'}\Omega_0(\langle \xi_{S_{j'}}\xi_{L_j}\rangle\phi + \langle \xi_{L_j}\xi_\Phi\rangle s_{j'}) + \kappa_j\Omega_0 P_j(\langle \xi_{S_j}\xi_\Phi\rangle\phi + \langle \xi_\Phi^2\rangle s_j)
\end{aligned} \tag{18}$$

ACKNOWLEDGMENT

This work was supported by a Sloan Research Fellowship to R.A. and by NIH grant 5-R01-A1053075-02 to E.H.

REFERENCES

1. J. D. Murray, *Mathematical Biology* (Springer-Verlag, New York, 1980).
2. R. Durrett and S. Levin, Importance of being discrete (and spatial), *Theor. Pop. Biol.* **46**:363–394 (1994).

3. T. M. Liggett, *Stochastic Interacting Systems: Contact, Voter and Exclusion Processes* (Springer, New York, 1999).
4. P. Rohani, D. J. Earn and B. T. Grenfell, Opposite patterns of synchrony in sympatric disease metapopulations, *Science* **286**:968–971 (1999).
5. O. N. Bjornstad and B. T. Grenfell, Noisy clockwork: Time series analysis of population fluctuations in animals, *Science* **293**:638–643 (2001).
6. M. E. J. Newman, Spread of epidemic disease on networks, *Phys. Rev. E* **66**:016128 (2002).
7. N. Grassly, C. Fraser and G. P. Garnett, Host immunity and synchronized epidemics of syphilis across the United States, *Nature* **433**:417–421 (2005).
8. N.S. Goel, S. C. Maitra and E. W. Montroll, On the Volterra and other nonlinear models of interacting populations, *Rev. Mod. Phys.* **43**:231–276 (1971).
9. A. J. McKane and T. J. Newman, Stochastic models in population biology and their deterministic analogs, *Phys. Rev. E* **70**:041902 (2004).
10. A. J. McKane and T. J. Newman, Predator-prey cycles from resonant amplification of demographic stochasticity, *Phys. Rev. Lett.* **94**:218102 (2005).
11. T. Park, Experimental studies of interspecific competition I. Competition between populations of the flour beetle, *Tribolium confusum* and Tribolium castaneum, *Ecol. Monogr.* **18**:267–307 (1948).
12. M. B. Bonsall and M. P. Hassell, Apparent competition structures ecological assemblages, *Nature* **388**:371–373 (1997).
13. P. Hudson and J. Greenman, Competition mediated by parasites: biological and theoretical progress, *TREE* **13**:387–390 (1998) and references therein.
14. F. Thomas, M. B. Bonsall and A. P. Dobson, Parasitism, biodiversity and conservation in F. Thomas, F. Renaud and J. F. Guegan (eds.) *Parasitism and Ecosystems* (Oxford University Press, Oxford, 2005).
15. R. D. Holt and J. Pickering, Infectious disease and species coexistence: a model of Lotka-Volterra form, *Am. Nat.* **125**:196–211 (1985).
16. M. Begon *et al*., Disease and community structure: the importance of host self-regulation in a host-host pathogen model, *Am. Nat.* **139**:1131–1150 (1992).
17. R. D. Holt and J. H. Lawton, The ecological consequences of shared natural enemies, *Annu. Rev. Ecol. Syst.* **25**:495–520 (1994).
18. R. G. Bowers and J. Turner, Community structure and the interplay between interspecific infection and competition, *J. Theor. Biol.* **187**:95–109 (1997).
19. J. V. Greenman and P. J. Hudson, Infected coexistence: instability with and without density-dependent regulation, *J. Theor. Biol.* **185**:345–356 (1997).
20. M. G. Weinbauer and F. Rassoulzadegan, Are viruses driving microbial diversification and diversity? *Environ. Microbiol.* **68**:2589–2594 (2004).
21. J. Joo, M. Gunny, M. Cases, P. Hudson, R. Albert and E. Harvill, Bacteriophage-mediated competition in *Bordetella* bacteria, *Proc. R. Soc. B* **273**:1843–1848 (2006).
22. P. A. Cotter and J. F. Miller, BvgAS-mediated signal tranduction: analysis of phage-locked regulatory mutants of *Bordetella bronchiseptica* in a rabbit model. *Infect. Immun.* **62**:3381–3390 (1994).
23. M. Liu *et al*., Genomic and genetic analysis of *Bordetella* bacteriophages encoding reverse transcriptase-mediated tropism-switching cassettes, *J. Bacteriol.* **186**:1503–1517 (2004).
24. M. Ptashne, *A Genetic Switch* (Cell Press and Blackwell Scientific Publications, Cambridge, 1992).
25. N. G. Van Kampen, *Stochastic Processes in Physics and Chemistry* (North-Holland, New York, 2001).
26. C. W. Gardiner, *Handbook of Stochastic Methods for Physics, Chemistry and Natural Sciences* (Springer-Verlag, Berlin, 2004).
27. D. T. Gillespie, Exact stochastic simulation of coupled chemical reactions, *J. Phys. Chem.* **81**:2340–2361 (1977).

28. David G. Kendall, On some modes of population growth leading to R. A. Fisher's logarithmic series distribution, *Biometrika* **35**:6–15 (1948).
29. L. E. Reichl, *A Modern Course in Statistical Physics* (University of Texas Press, Austin, 1980).
30. K. Kuulasmaa, The spatial general epidemic and locally dependent random graphs, *J. Appl. Probab.* **19**:745–758 (1982).
31. R. Durrett and C. Neuhauser, Epidemics with recovery in D 2, *Ann. Appl. Probab.* **1**:189–206 (1991).
32. E. Andjel and R. Schinazi, A complete convergence theorem for an epidemic model, *J. Appl. Probab.* **33**:741–748 (1996).
33. R. Pastor-Satorras and A. Vespignani, Epidemic spreading in scale-free networks, *Phys. Rev. Lett.* **86**:3200–3203 (2001).
34. S. M. Faruque, I. B. Naser, M. J. I. B. Islam, A. S. G. Faruque, A. N. Ghosh, G. B. Nair, D. A. Sack and J. J. Mekalanos, Seasonal epidemics of cholera inversely correlate with the prevalence of environmental cholera phages, *Proc. Natl. Acad. Sci.* **102**:1702 (2005).